Title
A Critical Analysis of Chemical and Electrochemical Oxidation Mechanisms in Li-Ion Batteries

Journal
The Journal of Physical Chemistry Letters, 15(2)

ISSN
1948-7185

Authors
Spotte-Smith, Evan Walter Clark
Vijay, Sudarshan
Petrocelli, Thea Bee
et al.

Publication Date
2024-01-18

DOI
10.1021/acs.jpclett.3c03279

Peer reviewed

THE JOURNAL OF PHYSICAL CHEMISTRY LETTERS
A JOURNAL OF THE AMERICAN CHEMICAL SOCIETY

pubs.acs.org/JPCL
Letter

A Critical Analysis of Chemical and Electrochemical Oxidation Mechanisms in Li-Ion Batteries

Evan Walter Clark Spotte-Smith, Sudarshan Vijay, Thea Bee Petrocelli, Bernardine L. D. Rinkel, Bryan D. McCloskey, and Kristin A. Persson*

Cite This: J. Phys. Chem. Lett. 2024, 15, 391−400

ABSTRACT: Electrolyte decomposition limits the lifetime of commercial lithium-ion batteries (LIBs) and slows the adoption of next-generation energy storage technologies. A fundamental understanding of electrolyte degradation is critical to rationally design stable and energy-dense LIBs. To date, most explanations for electrolyte decomposition at LIB positive electrodes have relied on ethylene carbonate (EC) being chemically oxidized by evolved singlet oxygen ($^1O_2$) or electrochemically oxidized. In this work, we apply density functional theory to assess the feasibility of these mechanisms. We find that electrochemical oxidation is unfavorable at any potential reached during normal LIB operation, and we predict that previously reported reactions between the EC and $^1O_2$ are kinetically limited at room temperature. Our calculations suggest an alternative mechanism in which EC reacts with superoxide (O_2^-) and/or peroxide (O_2^{2-}) anions. This work provides a new perspective on LIB electrolyte decomposition and motivates further studies to understand the reactivity at positive electrodes.

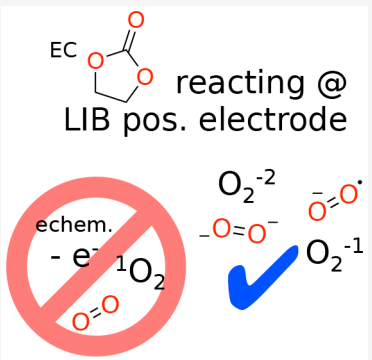

Electrolyte design is one of the most significant remaining challenges in the development of lithium-ion battery (LIB) technologies. To be practically useful, an electrolyte must simultaneously possess a number of key properties, including high Li^+ conductivity and transference number, low viscosity, and compatibility with the battery's positive and negative electrodes.[1] The latter requirement, that electrolytes must be stable at both electrodes, is especially challenging. To achieve a high energy density, LIBs operate at extreme potentials, as low as 0.1 V for common graphitic negative electrodes (in this work, all potentials are referenced to the reduction potential of Li^+) and, depending on the composition of the positive electrode, as high as 4.2−4.5 V for lithium nickel manganese cobalt oxides (NMC)[2] or 4.5−4.8 V for novel disordered rock salts (DRX).[3] In the reactive environment created at these potentials, most electrolytes tend to degrade over time, leading to decreased Coulombic efficiency and irreversible capacity loss.[4] To continue to improve the lifetime of LIBs and to enable the deployment of next-generation electrodes like DRX, it is essential either to prevent electrolyte decomposition reactions entirely or to promote the formation of passivation films, known as solid−electrolyte interphases (SEIs) when formed on the negative electrode[5] and cathode−electrolyte interphases (CEIs) when formed on the positive electrode.[6]

Commercial LIB electrolytes are solutions composed of lithium hexafluorophosphate ($LiPF_6$) dissolved in a mixture of organic carbonates, such as ethylene carbonate (EC) and ethyl methyl carbonate.[7,8] For many years, SEI formation mechanisms for carbonate/$LiPF_6$ electrolytes at LIB negative electrodes have been studied in detail; experimentally observed products have been mapped to reactants through a combination of experimental characterization techniques,[9,10] atomistic modeling,[11−13] and chemical reaction network (CRN) analysis.[14,15] By comparison, degradation mechanisms at positive electrodes have received less attention and are less well understood.

Electrochemical oxidation and chemical oxidation have been proposed in the literature as explanations for EC decomposition at potentials of $\gtrsim$4 V[16,17] (in general, exact onset potentials for electrolyte decomposition and other degradation processes depend on the electrode composition, among other factors).[18] In electrochemical oxidation, EC loses an electron to the electrode, after which it can react with other salt and solvent molecules.[19] Chemical oxidation does not involve direct electron transfer between the electrode and electrolyte but instead involves the attack by so-called "reactive oxygen". Diatomic oxygen (O_2) has been detected evolving at high potentials from transition metal oxide positive electrodes, including NMC (~4.2 V)[20,21] and DRX (~4.5 V).[22,23] Some reports studying NMC materials claim that this O_2 is released

Received: November 21, 2023
Revised: December 19, 2023
Accepted: December 27, 2023
Published: January 4, 2024

https://doi.org/10.1021/acs.jpclett.3c03279
J. Phys. Chem. Lett. 2024, 15, 391−400

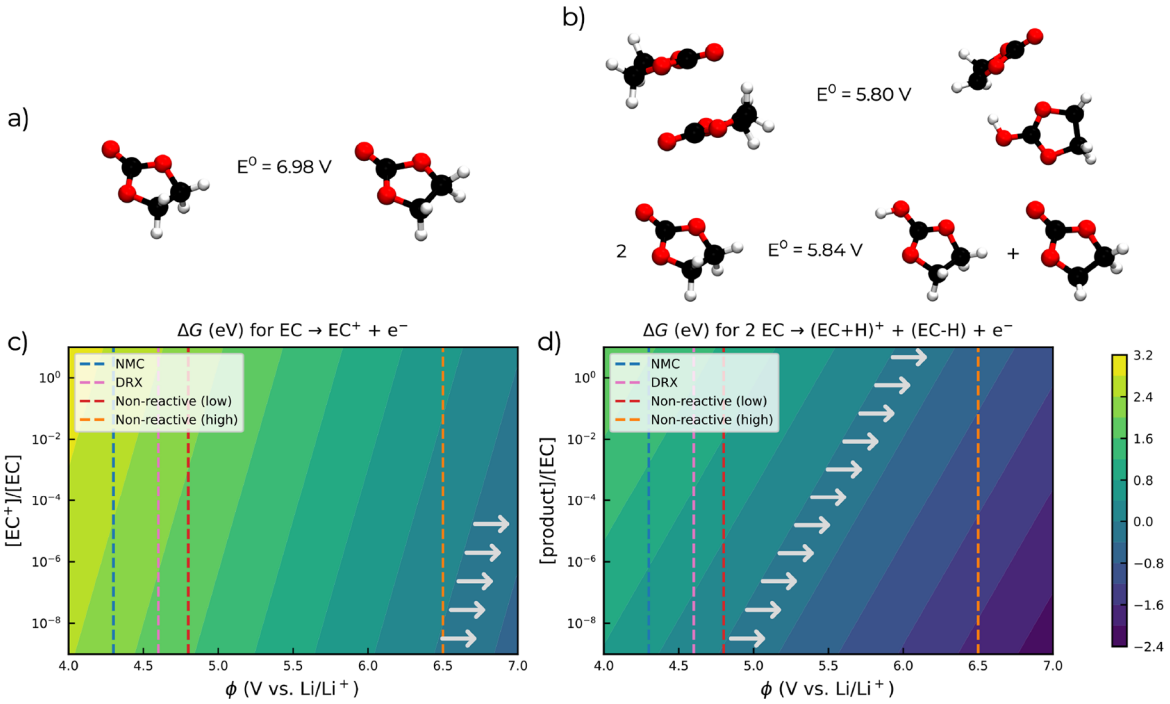

Figure 1. (a) Depiction of the oxidation reaction EC → $EC^+ + e^-$ (reaction 1), with three-dimensional (3D) structures for EC and EC^+. (b) Depictions of the concerted dissociative oxidation reaction 2EC → $(EC+H)^+ + (EC-H) + e^-$ (reaction 2), with 3D structures of the reactants and products as clusters (top) and isolated molecules (bottom). (c) Free energy change ΔG for the stepwise electrochemical oxidation of EC (reaction 1), as a function of potential and relative concentration. (d) ΔG for the concerted dissociative oxidation of EC (Reaction 2) as a function of potential and relative concentration, where we assume that $(EC+H)^+$ and EC−H are at the same concentration, denoted as [product]. Vertical lines in panels c and d indicate typical maximum potentials, for example, NMC (blue, shown at 4.3 V) and DRX (pink, shown at 4.6 V) positive electrodes, as well as the range of reported electrochemical oxidation potentials of EC at nonreactive electrodes (red and orange). For all points to the right of the arrow tails (at the ΔG = 0.0 eV line), electrochemical EC oxidation is predicted to be thermodynamically accessible.

in the singlet excited state ($^1O_2$),[10,24−27] which is considered to be more reactive than the triplet ground state ($^3O_2$).[28,29]

In this work, we evaluate both of these proposed reaction mechanisms using density functional theory (DFT) calculations. We show that electrochemical oxidation of EC is unlikely to occur at typical operating voltages in LIBs and that chemical oxidation by singlet oxygen is potentially also infeasible due to sluggish kinetics. These findings suggest that the potential-dependent degradation of EC at LIB positive electrodes occurs via alternate mechanisms. We conclude by hypothesizing a decomposition route that requires neither electrochemical oxidation nor reactions with $^1O_2$. Specifically, on the basis of the observations of partial oxygen redox to peroxide (O_2^{2-}) or "peroxo-like" species in transition metal oxide electrodes and reports of reactions between organic carbonates and superoxide anions (O_2^-), we suggest that oxygen anions may favorably react with and degrade EC.

We begin by considering electrochemical oxidation. The hypothesis that EC reacts electrochemically at battery positive electrodes appears suspect on the basis of the available experimental literature. Reported oxidation potentials for EC vary, but if we limit our consideration to measurements made using nonreactive electrodes such as platinum or glassy carbon, aiming to eliminate the possibility of reactions between EC and electrode surfaces, the reported values are between 4.8 and 6.5 V.[16,30−34] Even the low end of this range is considerably higher than typical LIB operating potentials. However, Chen[35] recently suggested that concentration effects may decrease the effective oxidation potential of EC. That is, if the products of electrochemical oxidation are sufficiently short-lived or in sufficiently low concentration at steady state, the reaction could become favorable at potentials below EC's standard oxidation potential.

To evaluate the possibility of electrochemical EC oxidation, we consider the elementary steps of charge transfer to EC. In the simplest mechanism, EC is oxidized as

$$EC \rightarrow EC^+ + e^- \quad (1)$$

where e^- is an electron and EC^+ is the oxidized form of EC (see Figure 1a). Our computations (see the Supporting Information for computational methods) show that this reaction has a standard oxidation potential E° of 6.98 V, which is significantly higher than the experimentally measured range.

The mechanism of EC oxidation may change when additional solvent molecules are involved. Xing and Borodin[19] previously applied DFT and Møller−Plesset perturbation theory to study the oxidation of a cluster of two EC molecules, EC_2. They found that, during the optimization of the oxidized cluster EC_2^+, a proton transferred from one EC to the other, making the reaction overall

$$2EC \rightarrow (EC+H)^+ + (EC-H) + e^- \quad (2)$$

This spontaneous transfer of a proton implies that the initial elementary step of electrochemical EC oxidation is a concerted reaction involving both charge transfer and proton transfer. We confirm that during DFT optimization of EC_2^+, proton transfer occurs, though this does not necessarily imply that EC oxidation is concerted. The calculated standard oxidation potential for reaction 2 is E° = 5.80 V using the free energies of

https://doi.org/10.1021/acs.jpclett.3c03279
J. Phys. Chem. Lett. 2024, 15, 391−400

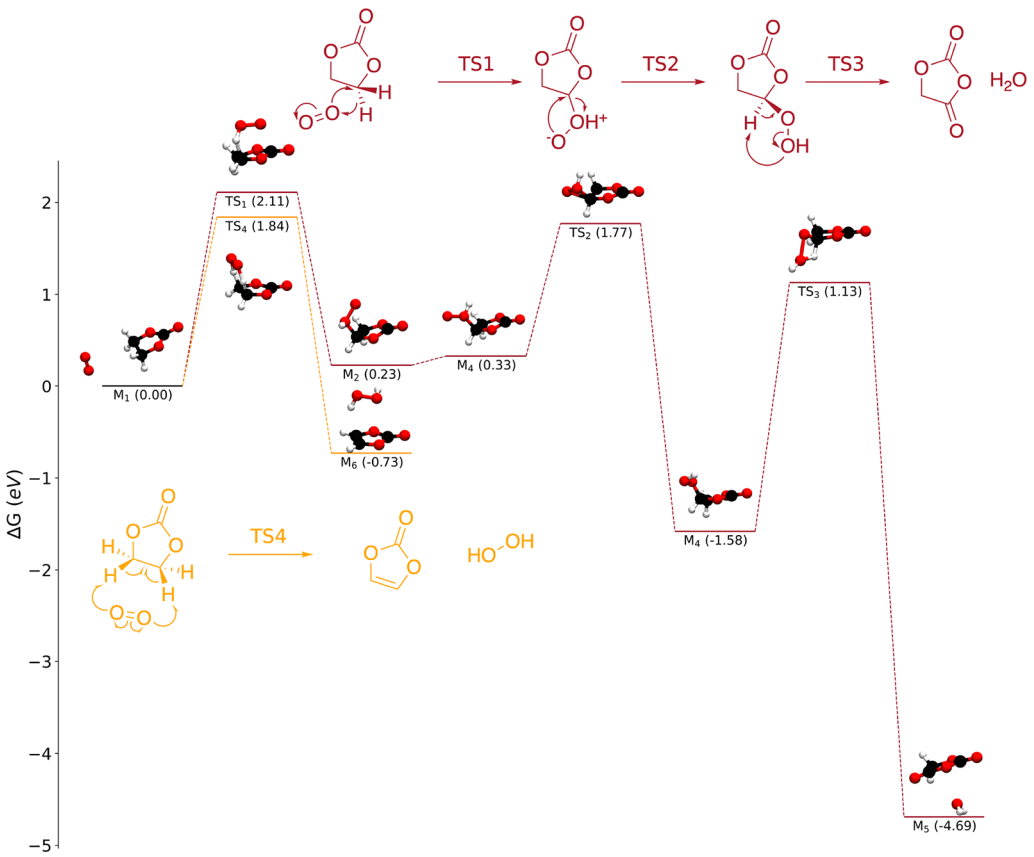

Figure 2. Energy diagrams for two reactions between $^1O_2$ and EC: a multistep reaction that eventually forms H_2O and a dicarbonyl species (red) and one in which $^1O_2$ abstracts two hydrogen atoms from EC to form H_2O_2 and vinylene carbonate (VC) in a single concerted step (yellow). Both pathways are thermodynamically favorable but severely kinetically limited.

the reactant and product clusters (Figure 1b, top) and E° = 5.84 V using reactants and products at infinite separation (Figure 1b, bottom), within the experimentally measured range at nonreactive electrodes.

Especially in the condensed phase, it can be difficult to determine if electron transfer reactions are stepwise (with charge transfer followed by additional bond cleavage and formation steps) or concerted.[36] Even if intermediates form following charge transfer in a stepwise mechanism, those intermediates may be too short-lived or at overly low concentrations to be experimentally observed. Although the calculated standard oxidation potential of the concerted dissociative oxidation given by reaction 2 is in better agreement with experimental characterization compared to that of reaction 1, we cannot at present say with certainty if electrochemical EC oxidation follows a stepwise or concerted pathway. This is especially true given Chen's argument about concentration effects. Given this uncertainty, we must consider both stepwise and concerted dissociative electrochemical EC oxidation.

To determine whether electrochemical oxidation is feasible under battery operating conditions, we compute the free energy change (ΔG) as

$$\Delta G = \Delta G^\circ + RT\ln(Q) - F\Delta\phi \tag{3}$$

where ΔG° is the free energy change under standard temperature, pressure, and concentration conditions at a fixed standard potential ϕ_0, R is the ideal gas constant, T is the absolute temperature in kelvin, Q is the reaction quotient, which is

$$Q = \frac{[EC^+]}{[EC]} \tag{4}$$

for the stepwise oxidation given by reaction 1 and

$$Q = \frac{[(EC{+}H)^+][(EC{-}H)]}{[EC]^2} \tag{5}$$

for the concerted dissociative oxidation given by reaction 2, F is Faraday's constant, and $\Delta\phi = \phi - \phi_0$ is the difference between the potential at the positive electrode and the reference potential. Here, we use the vacuum potential of the electron as ϕ_0.[37]

Neither the stepwise nor the concerted dissociative electrochemical oxidation reactions are feasible under the standard conditions, with standard oxidation potentials being significantly higher than 5 V. However, as indicated in eq 3, the feasibility of reactions 1 and 2 depends on both operating potential ϕ and the relative steady-state concentrations of the oxidation products.

Figure 1 shows ΔG for different ϕ values (x-axis) and relative concentrations (y-axis) for the stepwise (c) and concerted (d) mechanisms. The lower the relative concentration (along the y-axis for a fixed x-axis value), the greater the favorability of the reaction. Likewise, the reaction is more favorable as the potential is increased (along the x-axis for a fixed y-axis value).

https://doi.org/10.1021/acs.jpclett.3c03279
J. Phys. Chem. Lett. 2024, 15, 391−400

At all relative concentrations considered (as low as 10^{-9}), we predict that a potential of >6 V would need to be applied for reaction 1 to be thermodynamically favorable. Even considering possible error in our DFT calculations, this strongly suggests that the stepwise electrochemical oxidation of EC is not the dominant mechanism of EC degradation at LIB positive electrodes during normal battery operation. Because the standard oxidation potential of reaction 2 is considerably lower than that of reaction 1, concerted dissociative oxidation is more favorable at all potentials considered. The effect of relative concentration is also more significant in reaction 2, which involves two products (see eq 5). As such, Figure 1d shows that it could be possible for concerted dissociative EC oxidation to occur at applied potentials as low as ∼4.8 V. If the concerted dissociative mechanism is possible in real LIB electrolytes and the steady-state product concentrations are extremely low, it may be possible for electrochemical EC oxidation to occur at some high-voltage positive electrodes. However, even in this case, we predict that electrochemical oxidation cannot occur at lower potentials used with, e.g., NMC electrodes.

As we predicted that electrochemical oxidation of EC is unlikely to occur at applied potentials relevant to LIB operation, we now study the feasibility of chemical oxidation by $^1O_2$. We compute the free energies and free energy barriers for reaction mechanisms previously proposed in the literature, all taken at room temperature (298.15 K).

We identified two elementary mechanisms for chemical reactions between $^1O_2$ and EC (Figure 2). In the first (red) pathway, originally suggested by Jung et al.,[24] $^1O_2$ initially reacts with EC to form water and 1,3-dioxolane-2,4-dione, a dicarbonyl species. The second (yellow) pathway, proposed by Freiberg et al.,[38] results in the formation of H_2O_2 and vinylene carbonate (VC).

The water-forming pathway begins ($M_1 \rightarrow M_2$; $\Delta G^{\ddagger} = 2.11$ eV) with $^1O_2$ abstracting a hydrogen atom and attaching to the EC in a concerted reaction. The result of this attachment is the zwitterionic complex M_2. After rotation ($M_2 \rightarrow M_3$; $\Delta G = 0.10$ eV), a rearrangement occurs ($M_3 \rightarrow M_4$; $\Delta G^{\ddagger} = 1.44$ eV), replacing the zwitterionic −OHO group with a hydroperoxide group (−OOH). We note that we considered a direct reaction between M_1 and M_4, but all attempts to locate a transition state for the $M_1 \rightarrow M_4$ reaction resulted in optimizing the $M_1 \rightarrow M_2$ or $M_3 \rightarrow M_4$ transition state. In the final step ($M_4 \rightarrow M_5$; $\Delta G^{\ddagger} = 2.71$ eV), water is eliminated, leaving a carbonyl group. While this pathway is overall thermodynamically favorable ($M_1 \rightarrow M_5$; $\Delta G = -4.69$ eV), it is severely kinetically limited, with all three free energy barriers being >1.0 eV and two of the three being >2.0 eV. To exemplify the sluggish kinetics, consider the $M_1 \rightarrow M_2$ reaction proceeding at room temperature in a pure EC solution (concentration of ≈15 M) with a dissolved $^1O_2$ concentration of 1.56 mM (the solubility of O_2 in EC is discussed in the Supporting Information). Calculating the rate as

$$\text{rate} = k[\text{EC}][^1\text{O}_2] \tag{6}$$

where k is the rate coefficient of the reaction, determined using the Eyring equation

$$k = \frac{k_B T}{h} \exp\left(\frac{-\Delta G^{\ddagger}}{k_B T}\right) \tag{7}$$

we predict that the initial rate for this reaction (rate_0) would be 3.12×10^{-25} M s^{-1}, which is vanishingly small.

We note that previous studies have suggested that EC chemical oxidation does not end with elimination of a single H_2O molecule. Following this initial chemical oxidation, Jung et al. suggested that further oxidation by $^1O_2$ could result in the evolution of CO_2 and CO,[24] while Rinkel et al. proposed an alternative pathway to CO_2 and glycolic acid.[10] However, given that even the first step of the reaction between EC and $^1O_2$ is highly unlikely to occur, we have chosen not to pursue these downstream reaction pathways.

Compared to the water-forming pathway, the H_2O_2-forming pathway is more straightforward. In a single, concerted step, $^1O_2$ abstracts two hydrogen atoms from the ethylene carbons in the EC ($M_1 \rightarrow M_6$; $\Delta G^{\ddagger} = 1.84$ eV), yielding H_2O_2 and vinylene carbonate (VC). This mechanism is also thermodynamically favorable, with a ΔG of −0.73 eV, but due to the high barrier, we do not expect it to occur appreciably at room temperature ($\text{rate}_0 = 1.15 \times 10^{-20}$ M s^{-1}). We note that previous computational studies have indicated that the EC + $^1O_2 \rightarrow H_2O_2$ + VC reaction is kinetically limited. Using the complete active space second-order perturbation theory (CASPT2) multireference method with ANO-L-VDZP basis set in vacuum with the zero-point energy obtained from DFT, Freiberg et al.[38] predicted a reaction energy barrier ($\Delta E^{\ddagger}$) of 1.27 eV. Although we cannot directly compare our predictions with these values, as we performed our calculations in an implicit solvent medium and included enthalpic and entropic terms to calculate a free energy barrier, we can nonetheless say that our prediction agrees qualitatively with the result of Freiberg et al. in that they are significantly larger than what would be expected for a fast reaction.

We have not exhaustively considered all possible reactions between EC and $^1O_2$, but these findings suggest that $^1O_2$ may not be as reactive in the presence of EC as had previously been believed. While potentially surprising, the notion that reactions between EC and $^1O_2$ are kinetically limited appears to be consistent with the most direct evidence of such reactions. Freiberg et al.[38] fully saturated a solution of EC with O_2 and illuminated rose Bengal, a salt that can photochemically excite $^3O_2$ to $^1O_2$, continuously for 1 h to generate $^1O_2$ to react with EC. Using online electrochemical mass spectroscopy, they observed that some O_2 was consumed during the illumination of rose Bengal, on the order of tens of nanomoles for a milliliter sample of EC. They also observed the formation of H_2O_2 through colorimetry. Notably, the experiments of Freiberg et al. were performed at 45 °C, which should accelerate the reactions between EC and photogenerated $^1O_2$; despite this, the reaction appears to be slow.

More recently, Rinkel et al. performed similar experiments using O_2-saturated EC solutions and rose Bengal that were designed to promote chemical oxidation of EC.[27] After illumination for 2 h, relatively little reactivity between EC and $^1O_2$ was observed. Using solution-phase nuclear magnetic resonance (NMR) spectroscopy, the authors found that the amount of water in the solution increased by a factor of ∼3, which indicates some reactions took place in the saturated solution. However, the authors began with an electrolyte with a water content of <10 ppm, which means that the absolute quantity of water formed was minimal. Moreover, Rinkel et al. were unable to detect other expected reaction products, such as vinylene carbonate (VC) and hydrogen peroxide (H_2O_2),

https://doi.org/10.1021/acs.jpclett.3c03279
J. Phys. Chem. Lett. 2024, 15, 391−400

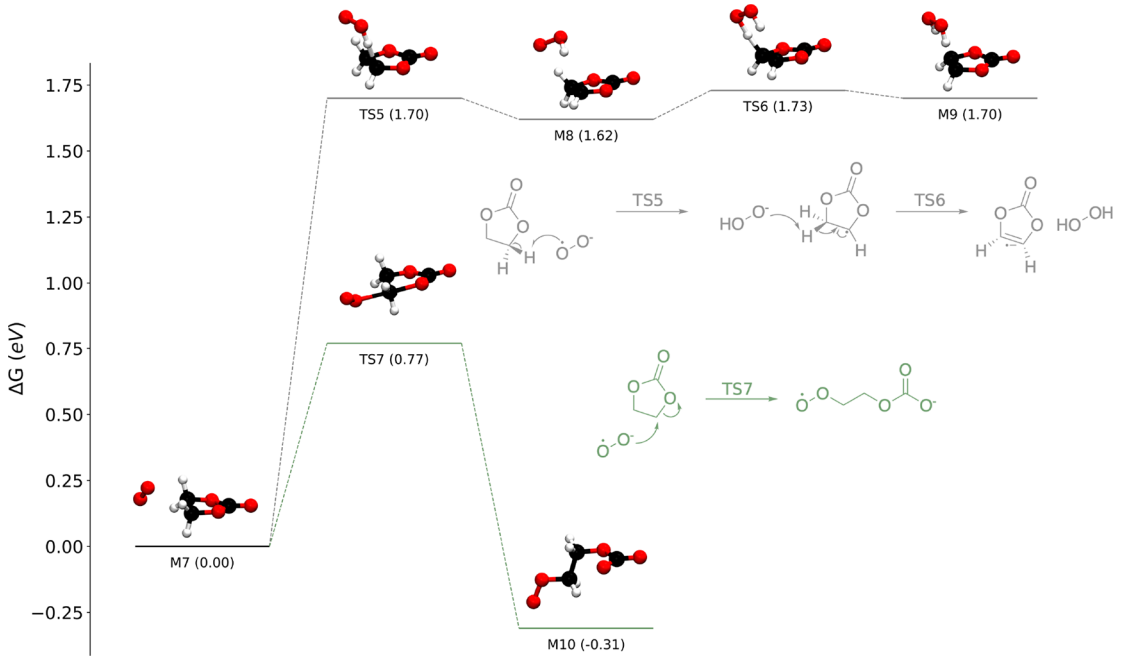

Figure 3. Energy diagrams for reactions between EC and superoxide (O_2^-), including a route forming H_2O_2 and reduced VC (gray) and a nucleophilic substitution (green).

though as Freiberg et al. note,[38] even if VC formed, it may be difficult to detect by NMR due to its low concentration and relative instability. In summary, reactions between $^1O_2$ and EC probably occur to some degree, but we believe that they are not the major drivers of electrolyte decomposition at LIB positive electrodes.

As our calculations call into question the electrochemical as well as chemical oxidation of EC at LIB positive electrodes, we find it necessary to consider alternative mechanisms for the observed reactivity of EC at increased potentials. We propose one such alternative, that EC may indeed combine with "reactive oxygen", but that the "reactive oxygen" is comprised of oxygen anions superoxide (O_2^-) and/or peroxide (O_2^{2-}), rather than $^1O_2$. This explanation is consistent with the existing literature on oxygen in LIB positive electrodes. It is well-known that oxygen redox occurs within many oxide positive electrodes during battery charging and discharging.[39−43] Both experimental and theoretical studies have observed peroxides or "peroxo-like" oxygen dimers in the electrode bulk.[44−46] These dimers have been suggested as intermediates that can eventually lead to neutral O_2 evolution. More recently, Genreith-Schriever et al.[47] performed *ab initio* molecular dynamics simulations on $LiNiO_2$ electrodes and showed that peroxide dimers form on the electrode surface, which is more directly related to oxygen loss and reactions with electrolyte molecules. Moreover, superoxide species are believed to be important intermediates in metal−air batteries, where they have been linked to the decomposition of carbonate solvents.[48−50]

As with $^1O_2$, we identified a number of elementary reaction mechanisms between EC and either O_2^- (Figure 3) or O_2^{2-} (Figure 4) using DFT. It is worth noting that these mechanisms are only suggestions of the initial steps of EC decomposition, and further work must be done to examine how these reactions may lead to more stable decomposition products.

We find that O_2^- cannot abstract protons or hydrogen atoms from EC to form H_2O_2. The first hydrogen abstraction ($M_7 \rightarrow M_8$) suffers from a high free energy barrier ($\Delta G^{\ddagger}$ = 1.70 eV) and is thermodynamically unfavorable (ΔG = 1.62 eV). The removal of an additional proton to form H_2O_2 and reduced radical VC is also somewhat unfavorable ($M_8 \rightarrow M_9$; ΔG = 0.08 eV) but has a modest barrier of 0.11 eV.

While O_2^- may not be able to attack EC's protons, it can attack the ethylene carbons, in agreement with previous studies focused on Li−O_2 batteries.[51] We identified a nucleophilic substitution reaction ($M_7 \rightarrow M_{10}$). This reaction is favorable (ΔG = −0.31 eV), and while it is not predicted to be rapid ($\Delta G^{\ddagger}$ = 0.77 eV), it is considerably faster than any $^1O_2$ reaction that we have identified. For comparison, if we consider the same conditions as we did previously (O_2^- at the saturation concentration of O_2 dissolved in pure EC at room temperature), the initial rate for the $M_7 \rightarrow M_{10}$ reaction ($rate_0$) is predicted to be 0.014 M s^{-1}, more than 20 orders of magnitude faster than the $M_1 \rightarrow M_2$ reaction. Aside from the predicted energy barrier, the $M_7 \rightarrow M_{10}$ reaction appears to be plausible on the basis of previous experimental observations. Specifically, Kaufman and McCloskey recently used differential electrochemical mass spectroscopy to detect electrolyte decomposition products that formed at lithium-excess NMC electrodes;[21] they observed peroxide-containing products related to M_{10} and even hypothesized that such species could form via nucleophilic substitution.

Reactions with peroxide are even more facile. Whereas proton abstraction is unfavorable for superoxide, it is predicted to occur rapidly for peroxide ($M_{11} \rightarrow M_{12}$; $\Delta G^{\ddagger}$ = 0.08 eV). Similarly, nucleophilic attack on the ethylene carbons of EC by O_2^{2-} is extremely favorable and rapid ($M_{11} \rightarrow M_{13}$; ΔG = −2.72 eV; $\Delta G^{\ddagger}$ = 0.17 eV). Finally, we predict that peroxide can attach to the carbonate carbon of EC, forming a tetrahedral complex ($M_{11} \rightarrow M_{14}$; $\Delta G^{\ddagger}$ = 0.38 eV).

Here, we have used first-principles DFT calculations to examine common explanations for high-potential electrolyte

https://doi.org/10.1021/acs.jpclett.3c03279
J. Phys. Chem. Lett. 2024, 15, 391−400

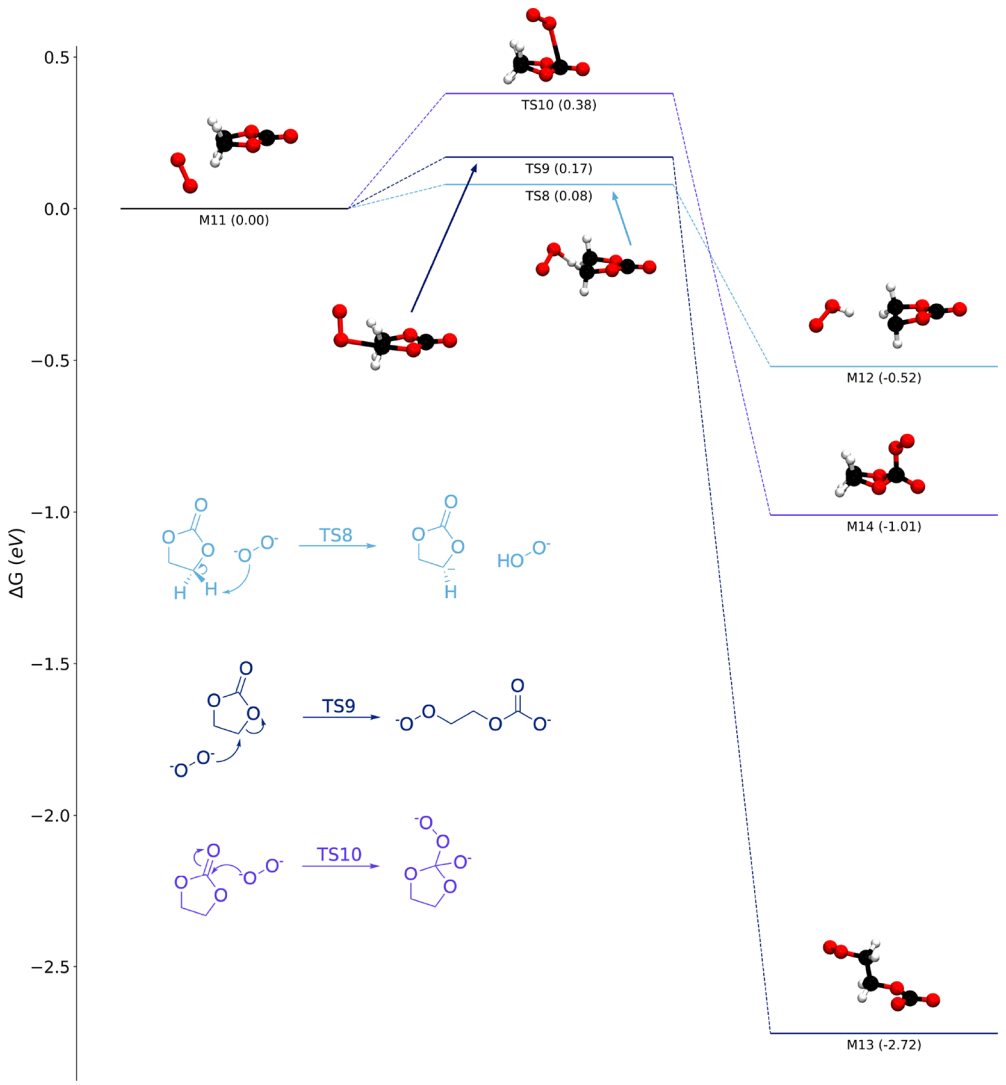

Figure 4. Energy diagrams for reactions between EC and peroxide (O_2^{2-}): proton abstraction (light blue), nucleophilic substitution (dark blue), and addition to form a tetrahedral complex (purple).

degradation in LIBs, focusing on model EC-based electrolytes. Even after accounting for the effect of concentration, we found that purely electrochemical oxidation of EC is thermodynamically disfavored at essentially any potential relevant to normal LIB operation. We likewise cast doubt on hypotheses related to $^1O_2$, as both of the major reactions reported in the literature are predicted to have large kinetic barriers, making them sluggish under ambient conditions.

On the basis of previous studies of oxygen redox in LIB positive electrodes, we suggest the possibility that EC may react with oxygen anions instead of neutral $^1O_2$. These anionic species are likely to be formed on transition metal oxide surfaces as an intermediate prior to neutral release of the O_2. Our initial calculations show that EC can react rapidly with O_2^- and especially O_2^{2-}. Additional studies, both computational and experimental, should now be undertaken to assess (i) how easily these anion species can form on NMC, DRX, or other oxide electrode surfaces, (ii) the lifetime of these anions, and (iii) if they can be eliminated from the electrode surface to react homogeneously with the electrolyte, as we have assumed here. We emphasize that in this work we have considered only the initial reactions between EC and oxygen anions. Even if they do occur, we do not yet know if these reactions can lead to observed products, such as water and acids, or what other products and intermediates may be formed. In the future, we intend to use CRN-based methods to more thoroughly explore reactions between EC and oxygen anions.

In this study, we largely ignored the role of electrode surfaces, treating the electrode mainly as a sink for electrons or as a source of various "reactive oxygen" species. However, electrode active material may also directly participate in reactions with electrolyte components such as EC or may act as catalysts. For instance, it has been suggested that EC is dehydrogenated on transition metal oxides.[27,34,52] While some initial studies of electrolyte reactions with oxide positive electrodes have been conducted using DFT,[53−55] they have typically been limited to examining a small number of reactions or performing very short dynamic simulations on the picosecond time scale. We hope that further computational studies consider the possible reactive and catalytic nature of LIB positive electrodes in more detail.

We likewise largely ignored salts such as $LiPF_6$, choosing to focus on solvent reactivity. Salt anions may also react at increased potentials,[56,57] and it has been suggested that EC and

https://doi.org/10.1021/acs.jpclett.3c03279
J. Phys. Chem. Lett. 2024, 15, 391−400

PF_6^- react together at LIB positive electrodes, forming products such as HF.[58,59] A complete understanding of LIB electrolyte reactivity at positive electrodes will require additional studies of reaction mechanisms, including salt molecules.

Finally, for the purposes of simplicity and computational cost, we have mostly neglected the role of explicit solvation shells in this work. As strong solvent effects have been identified for particular electrolyte decomposition reactions,[60] we cannot discount the possibility that the reactions reported here may be accelerated by particular solvent environments. Calculations involving complete solvent clusters should be performed to determine if or how explicit solvation affects reactions between EC and $^1O_2$, O_2^-, or O_2^{2-}.

■ ASSOCIATED CONTENT

Supporting Information

The Supporting Information is available free of charge at https://pubs.acs.org/doi/10.1021/acs.jpclett.3c03279.

Software availability, data availability, computational methods, calculation of the solubility of O_2 in EC, and cited refs 61−72 (PDF)

Transparent Peer Review report available (PDF)

■ AUTHOR INFORMATION

Corresponding Author

Kristin A. Persson − *Department of Materials Science and Engineering, University of California, Berkeley, Berkeley, California 94720, United States; Molecular Foundry, Lawrence Berkeley National Laboratory, Berkeley, California 94720, United States;* orcid.org/0000-0003-2495-5509; Email: kapersson@lbl.gov

Authors

Evan Walter Clark Spotte-Smith − *Department of Materials Science and Engineering, University of California, Berkeley, Berkeley, California 94720, United States; Materials Science Division, Lawrence Berkeley National Laboratory, Berkeley, California 94720, United States;* orcid.org/0000-0003-1554-197X

Sudarshan Vijay − *Department of Materials Science and Engineering, University of California, Berkeley, Berkeley, California 94720, United States;* Present Address: VASP Software GmbH, Sensengasse 8, Vienna A-1090, Austria

Thea Bee Petrocelli − *Department of Materials Science and Engineering, University of California, Berkeley, Berkeley, California 94720, United States*

Bernardine L. D. Rinkel − *Department of Chemical and Biomolecular Engineering, University of California, Berkeley, Berkeley, California 94720, United States; Energy Storage and Distributed Resources, Lawrence Berkeley National Laboratory, Berkeley, California 94720, United States*

Bryan D. McCloskey − *Department of Chemical and Biomolecular Engineering, University of California, Berkeley, Berkeley, California 94720, United States; Energy Storage and Distributed Resources, Lawrence Berkeley National Laboratory, Berkeley, California 94720, United States;* orcid.org/0000-0001-6599-2336

Complete contact information is available at: https://pubs.acs.org/10.1021/acs.jpclett.3c03279

Author Contributions

E.W.C.S.-S. and S.V. contributed equally to this work. E.W.C.S.-S.: conceptualization, formal analysis, funding acquisition, investigation, methodology, supervision, visualization, writing of the original draft, and review and editing. S.V.: conceptualization, formal analysis, investigation, methodology, visualization, writing of the original draft, and review and editing. T.B.P.: investigation. B.L.D.R.: conceptualization and review and editing. B.D.M.: funding acquisition and supervision. K.A.P.: funding acquisition, resources, supervision, and review and editing.

Notes

The authors declare no competing financial interest.

■ ACKNOWLEDGMENTS

E.W.C.S.-S. was supported by the Kavli Energy NanoScience Institute Philomathia Graduate Student Fellowship. S.V. was supported by the Betty and Gordon Moore Foundation. T.B.P. conducted this work as part of the Community College Internship program under the U.S. Department of Energy, Office of Science, Office of Workforce Development for Teachers and Scientists. Additional support comes from the Silicon Consortium Project (SCP) directed by Brian Cunningham under the Assistant Secretary for Energy Efficiency and Renewable Energy, Office of Vehicle Technologies of the U.S. Department of Energy (Contract DE-AC02-05CH11231), as well as the Disordered Rock Salt Consortium (DRX+) program directed by Tien Duong under the Assistant Secretary for Energy Efficiency and Renewable Energy, Office of Vehicle Technologies of the U.S. Department of Energy (Contract DE-AC02-05CH11231). The authors thank M. Rohith Srinivaas for useful discussions.

■ REFERENCES

(1) Xu, K. Nonaqueous Liquid Electrolytes for Lithium-Based Rechargeable Batteries. *Chem. Rev.* **2004**, *104*, 4303−4418.

(2) Heiskanen, S. K.; Laszczynski, N.; Lucht, B. L. Perspective — Surface Reactions of Electrolyte with LiNixCoyMnzO2 Cathodes for Lithium Ion Batteries. *J. Electrochem. Soc.* **2020**, *167*, 100519.

(3) Wang, M.; Chen, X.; Yao, H.; Lin, G.; Lee, J.; Chen, Y.; Chen, Q. Research Progress in Lithium-Excess Disordered Rock-Salt Oxides Cathode. *Energy & Environmental Materials* **2022**, *5*, 1139−1154.

(4) Xu, K. Electrolytes and Interphases in Li-Ion Batteries and Beyond. *Chem. Rev.* **2014**, *114*, 11503−11618.

(5) Winter, M. The Solid Electrolyte Interphase — The Most Important and the Least Understood Solid Electrolyte in Rechargeable Li Batteries. *Zeitschrift für Physikalische Chemie* **2009**, *223*, 1395−1406.

(6) Kühn, S. P.; Edström, K.; Winter, M.; Cekic-Laskovic, I. Face to Face at the Cathode Electrolyte Interphase: From Interface Features to Interphase Formation and Dynamics. *Adv. Mater. Interfaces* **2022**, *9*, 2102078.

(7) Blomgren, G. E. Electrolytes for Advanced Batteries. *J. Power Sources* **1999**, *81−82*, 112−118.

(8) Zhang, S. S.; Jow, T. R.; Amine, K.; Henriksen, G. L. LiPF6−EC−EMC Electrolyte for Li-Ion Battery. *J. Power Sources* **2002**, *107*, 18−23.

(9) Nie, M.; Chalasani, D.; Abraham, D. P.; Chen, Y.; Bose, A.; Lucht, B. L. Lithium Ion Battery Graphite Solid Electrolyte Interphase Revealed by Microscopy and Spectroscopy. *J. Phys. Chem. C* **2013**, *117*, 1257−1267.

(10) Rinkel, B. L. D.; Hall, D. S.; Temprano, I.; Grey, C. P. Electrolyte Oxidation Pathways in Lithium-Ion Batteries. *J. Am. Chem. Soc.* **2020**, *142*, 15058−15074.

(11) Wang, Y.; Nakamura, S.; Ue, M.; Balbuena, P. B. Theoretical Studies To Understand Surface Chemistry on Carbon Anodes for Lithium-Ion Batteries: Reduction Mechanisms of Ethylene Carbonate. *J. Am. Chem. Soc.* **2001**, *123*, 11708−11718.
(12) Kuai, D.; Balbuena, P. B. Solvent Degradation and Polymerization in the Li-Metal Battery: Organic-Phase Formation in Solid-Electrolyte Interphases. *ACS Appl. Mater. Interfaces* **2022**, *14*, 2817−2824.
(13) Spotte-Smith, E. W. C.; Petrocelli, T. B.; Patel, H. D.; Blau, S. M.; Persson, K. A. Elementary Decomposition Mechanisms of Lithium Hexafluorophosphate in Battery Electrolytes and Interphases. *ACS Energy Letters* **2023**, *8*, 347−355.
(14) Barter, D.; Clark Spotte-Smith, E. W.; Redkar, N. S.; Khanwale, A.; Dwaraknath, S.; Persson, K. A.; Blau, S. M. Predictive Stochastic Analysis of Massive Filter-Based Electrochemical Reaction Networks. *Digital Discovery* **2023**, *2*, 123−137.
(15) Spotte-Smith, E. W. C.; Kam, R. L.; Barter, D.; Xie, X.; Hou, T.; Dwaraknath, S.; Blau, S. M.; Persson, K. A. Toward a Mechanistic Model of Solid−Electrolyte Interphase Formation and Evolution in Lithium-Ion Batteries. *ACS Energy Letters* **2022**, *7*, 1446−1453.
(16) Azcarate, I.; Yin, W.; Méthivier, C.; Ribot, F.; Laberty-Robert, C.; Grimaud, A. Assessing the Oxidation Behavior of EC:DMC Based Electrolyte on Non-Catalytically Active Surface. *J. Electrochem. Soc.* **2020**, *167*, No. 080530.
(17) Rowden, B.; Garcia-Araez, N. A Review of Gas Evolution in Lithium-Ion Batteries. *Energy Reports* **2020**, *6*, 10−18.
(18) Dose, W. M.; Li, W.; Temprano, I.; O'Keefe, C. A.; Mehdi, B. L.; De Volder, M. F.; Grey, C. P. Onset Potential for Electrolyte Oxidation and Ni-Rich Cathode Degradation in Lithium-Ion Batteries. *ACS Energy Lett.* **2022**, *7*, 3524−3530.
(19) Xing, L.; Borodin, O. Oxidation Induced Decomposition of Ethylene Carbonate from DFT Calculations — Importance of Explicitly Treating Surrounding Solvent. *Phys. Chem. Chem. Phys.* **2012**, *14*, 12838−12843.
(20) Fell, C. R.; Qian, D.; Carroll, K. J.; Chi, M.; Jones, J. L.; Meng, Y. S. Correlation Between Oxygen Vacancy, Microstrain, and Cation Distribution in Lithium-Excess Layered Oxides During the First Electrochemical Cycle. *Chem. Mater.* **2013**, *25*, 1621−1629.
(21) Kaufman, L. A.; McCloskey, B. D. Surface Lithium Carbonate Influences Electrolyte Degradation via Reactive Oxygen Attack in Lithium-Excess Cathode Materials. *Chem. Mater.* **2021**, *33*, 4170−4176.
(22) Luo, K.; Roberts, M. R.; Hao, R.; Guerrini, N.; Pickup, D. M.; Liu, Y.-S.; Edström, K.; Guo, J.; Chadwick, A. V.; Duda, L. C.; Bruce, P. G. Charge-Compensation in 3d-Transition-Metal-Oxide Intercalation Cathodes Through the Generation of Localized Electron Holes on Oxygen. *Nat. Chem.* **2016**, *8*, 684−691.
(23) Lun, Z.; Ouyang, B.; Kitchaev, D. A.; Clément, R. J.; Papp, J. K.; Balasubramanian, M.; Tian, Y.; Lei, T.; Shi, T.; McCloskey, B. D.; Lee, J.; Ceder, G. Improved Cycling Performance of Li-Excess Cation-Disordered Cathode Materials upon Fluorine Substitution. *Adv. Energy Mater.* **2019**, *9*, 1802959.
(24) Jung, R.; Metzger, M.; Maglia, F.; Stinner, C.; Gasteiger, H. A. Oxygen Release and Its Effect on the Cycling Stability of LiNixMnyCozO2 (NMC) Cathode Materials for Li-Ion Batteries. *J. Electrochem. Soc.* **2017**, *164*, A1361.
(25) Jung, R.; Metzger, M.; Maglia, F.; Stinner, C.; Gasteiger, H. A. Chemical versus Electrochemical Electrolyte Oxidation on NMC111, NMC622, NMC811, LNMO, and Conductive Carbon. *J. Phys. Chem. Lett.* **2017**, *8*, 4820−4825.
(26) Wandt, J.; Freiberg, A. T.; Ogrodnik, A.; Gasteiger, H. A. Singlet Oxygen Evolution from Layered Transition Metal Oxide Cathode Materials and its Implications for Lithium-Ion Batteries. *Mater. Today* **2018**, *21*, 825−833.
(27) Rinkel, B. L. D.; Vivek, J. P.; Garcia-Araez, N.; Grey, C. P. Two Electrolyte Decomposition Pathways at Nickel-Rich Cathode Surfaces in Lithium-Ion Batteries. *Energy Environ. Sci.* **2022**, *15*, 3416−3438.
(28) Clennan, E. L. New mechanistic and synthetic aspects of singlet oxygen chemistry. *Tetrahedron* **2000**, *56*, 9151−9179.
(29) Al-Nu'airat, J.; Oluwoye, I.; Zeinali, N.; Altarawneh, M.; Dlugogorski, B. Z. Review of chemical reactivity of singlet oxygen with organic fuels and contaminants. *Chem. Rec.* **2021**, *21*, 315−342.
(30) Ue, M.; Takeda, M.; Takehara, M.; Mori, S. Electrochemical Properties of Quaternary Ammonium Salts for Electrochemical Capacitors. *J. Electrochem. Soc.* **1997**, *144*, 2684.
(31) Xu, K.; Ding, S. P.; Jow, T. R. Toward Reliable Values of Electrochemical Stability Limits for Electrolytes. *J. Electrochem. Soc.* **1999**, *146*, 4172−4178.
(32) Abe, K.; Ushigoe, Y.; Yoshitake, H.; Yoshio, M. Functional Electrolytes: Novel Type Additives for Cathode Materials, Providing High Cycleability Performance. *J. Power Sources* **2006**, *153*, 328−335.
(33) Metzger, M.; Marino, C.; Sicklinger, J.; Haering, D.; Gasteiger, H. A. Anodic Oxidation of Conductive Carbon and Ethylene Carbonate in High-Voltage Li-Ion Batteries Quantified by On-Line Electrochemical Mass Spectrometry. *J. Electrochem. Soc.* **2015**, *162*, A1123−A1134.
(34) Zhang, Y.; Katayama, Y.; Tatara, R.; Giordano, L.; Yu, Y.; Fraggedakis, D.; Sun, J. G.; Maglia, F.; Jung, R.; Bazant, M. Z.; Shao-Horn, Y. Revealing Electrolyte Oxidation via Carbonate Dehydrogenation on Ni-Based Oxides in Li-Ion Batteries by in Situ Fourier Transform Infrared Spectroscopy. *Energy Environ. Sci.* **2020**, *13*, 183−199.
(35) Chen, Z. Chasing Protons in Lithium-Ion Batteries. *Chem. Commun.* **2022**, *58*, 10127−10135.
(36) Maletin, Y. A.; Cannon, R. D. Dissociative Electron Transfer Reactions. *Theor. Exp. Chem.* **1998**, *34*, 57−68.
(37) Trasatti, S. The Absolute Electrode Potential: An Explanatory Note (Recommendations 1986). *Pure Appl. Chem.* **1986**, *58*, 955−966.
(38) Freiberg, A. T. S.; Roos, M. K.; Wandt, J.; De Vivie-Riedle, R.; Gasteiger, H. A. Singlet Oxygen Reactivity with Carbonate Solvents Used for Li-Ion Battery Electrolytes. *J. Phys. Chem. A* **2018**, *122*, 8828−8839.
(39) Tarascon, J.; Vaughan, G.; Chabre, Y.; Seguin, L.; Anne, M.; Strobel, P.; Amatucci, G. In Situ Structural and Electrochemical Study of Ni1-xCoxO2Metastable Oxides Prepared by Soft Chemistry. *Journal of solid state chemistry* **1999**, *147*, 410−420.
(40) Lee, E.; Persson, K. A. Structural and Chemical Evolution of the Layered Li-Excess LixMnO3 as a Function of Li Content from First-Principles Calculations. *Adv. Energy Mater.* **2014**, *4*, 1400498.
(41) Wang, R.; Li, X.; Liu, L.; Lee, J.; Seo, D.-H.; Bo, S.-H.; Urban, A.; Ceder, G. A Disordered Rock-Salt Li-Excess Cathode Material with High Capacity and Substantial Oxygen Redox Activity: Li1.25Nb0.25Mn0.5O2. *Electrochem. Commun.* **2015**, *60*, 70−73.
(42) Grenier, A.; Kamm, G. E.; Li, Y.; Chung, H.; Meng, Y. S.; Chapman, K. W. Nanostructure Transformation as a Signature of Oxygen Redox in Li-Rich 3d and 4d Cathodes. *J. Am. Chem. Soc.* **2021**, *143*, 5763−5770.
(43) Huang, T.-Y.; Cai, Z.; Crafton, M. J.; Kaufman, L. A.; Konz, Z. M.; Bergstrom, H. K.; Kedzie, E. A.; Hao, H.-M.; Ceder, G.; McCloskey, B. D. Quantitative Decoupling of Oxygen-Redox and Manganese-Redox Voltage Hysteresis in a Cation-Disordered Rock Salt Cathode. *Adv. Energy Mater.* **2023**, *13*, 2300241.
(44) McCalla, E.; Abakumov, A. M.; Saubanère, M.; Foix, D.; Berg, E. J.; Rousse, G.; Doublet, M.-L.; Gonbeau, D.; Novák, P.; Van Tendeloo, G.; Dominko, R.; Tarascon, J.-M. Visualization of O-O peroxo-like dimers in high-capacity layered oxides for Li-ion batteries. *Science* **2015**, *350*, 1516−1521.
(45) Saubanère, M.; McCalla, E.; Tarascon, J.-M.; Doublet, M.-L. The Intriguing Question of Anionic Redox in High-Energy Density Cathodes for Li-Ion Batteries. *Energy Environ. Sci.* **2016**, *9*, 984−991.
(46) Hong, J.; Gent, W. E.; Xiao, P.; Lim, K.; Seo, D.-H.; Wu, J.; Csernica, P. M.; Takacs, C. J.; Nordlund, D.; Sun, C.-J.; Stone, K. H.; Passarello, D.; Yang, W.; Prendergast, D.; Ceder, G.; Toney, M. F.; Chueh, W. C. Metal−Oxygen Decoordination Stabilizes Anion Redox in Li-Rich Oxides. *Nat. Mater.* **2019**, *18*, 256−265.

https://doi.org/10.1021/acs.jpclett.3c03279
J. Phys. Chem. Lett. 2024, 15, 391−400

(47) Genreith-Schriever, A. R.; Banerjee, H.; Menon, A. S.; Bassey, E. N.; Piper, L. F.; Grey, C. P.; Morris, A. J. Oxygen Hole Formation Controls Stability in LiNiO2 Cathodes. *Joule* **2023**, *7*, 1623−1640.
(48) Yang, J.; Zhai, D.; Wang, H.-H.; Lau, K. C.; Schlueter, J. A.; Du, P.; Myers, D. J.; Sun, Y.-K.; Curtiss, L. A.; Amine, K. Evidence for Lithium Superoxide-Like Species in the Discharge Product of a Li−O2 Battery. *Phys. Chem. Chem. Phys.* **2013**, *15*, 3764−3771.
(49) Zhai, D.; Wang, H.-H.; Lau, K. C.; Gao, J.; Redfern, P. C.; Kang, F.; Li, B.; Indacochea, E.; Das, U.; Sun, H.-H.; Sun, H.-J.; Amine, K.; Curtiss, L. A. Raman Evidence for Late Stage Disproportionation in a Li−O2 Battery. *J. Phys. Chem. Lett.* **2014**, *5*, 2705−2710.
(50) Wang, Y.; Lu, Y.-R.; Dong, C.-L.; Lu, Y.-C. Critical Factors Controlling Superoxide Reactions in Lithium−Oxygen Batteries. *ACS Energy Letters* **2020**, *5*, 1355−1363.
(51) Bryantsev, V. S.; Giordani, V.; Walker, W.; Blanco, M.; Zecevic, S.; Sasaki, K.; Uddin, J.; Addison, D.; Chase, G. V. Predicting Solvent Stability in Aprotic Electrolyte Li−Air Batteries: Nucleophilic Substitution by the Superoxide Anion Radical (). *J. Phys. Chem. A* **2011**, *115*, 12399−12409.
(52) Giordano, L.; Karayaylali, P.; Yu, Y.; Katayama, Y.; Maglia, F.; Lux, S.; Shao-Horn, Y. Chemical Reactivity Descriptor for the Oxide-Electrolyte Interface in Li-Ion Batteries. *journal of physical chemistry letters* **2017**, *8*, 3881−3887.
(53) Kumar, N.; Leung, K.; Siegel, D. J. Crystal Surface and State of Charge Dependencies of Electrolyte Decomposition on LiMn2O4 Cathode. *J. Electrochem. Soc.* **2014**, *161*, E3059.
(54) Choi, D.; Kang, J.; Park, J.; Han, B. First-Principles Study on Thermodynamic Stability of the Hybrid Interfacial Structure of LiMn2O4 Cathode and Carbonate Electrolyte in Li-Ion Batteries. *Phys. Chem. Chem. Phys.* **2018**, *20*, 11592−11597.
(55) Xu, S.; Luo, G.; Jacobs, R.; Fang, S.; Mahanthappa, M. K.; Hamers, R. J.; Morgan, D. Ab Initio Modeling of Electrolyte Molecule Ethylene Carbonate Decomposition Reaction on $Li(Ni,Mn,Co)O_2$ Cathode Surface. *ACS Appl. Mater. Interfaces* **2017**, *9*, 20545−20553.
(56) Wagner, R.; Korth, M.; Streipert, B.; Kasnatscheew, J.; Gallus, D. R.; Brox, S.; Amereller, M.; Cekic-Laskovic, I.; Winter, M. Impact of Selected LiPF6 Hydrolysis Products on the High Voltage Stability of Lithium-Ion Battery Cells. *ACS Appl. Mater. Interfaces* **2016**, *8*, 30871−30878.
(57) Liu, M.; Vatamanu, J.; Chen, X.; Xing, L.; Xu, K.; Li, W. Hydrolysis of LiPF6-Containing Electrolyte at High Voltage. *ACS Energy Letters* **2021**, *6*, 2096−2102.
(58) Solchenbach, S.; Metzger, M.; Egawa, M.; Beyer, H.; Gasteiger, H. A. Quantification of PF5 and POF3 from Side Reactions of LiPF6 in Li-Ion Batteries. *J. Electrochem. Soc.* **2018**, *165*, A3022.
(59) Jayawardana, C.; Rodrigo, N.; Parimalam, B.; Lucht, B. L. Role of Electrolyte Oxidation and Difluorophosphoric Acid Generation in Crossover and Capacity Fade in Lithium Ion Batteries. *ACS Energy Letters* **2021**, *6*, 3788−3792.
(60) Boyer, M. J.; Hwang, G. S. Theoretical Prediction of the Strong Solvent Effect on Reduced Ethylene Carbonate Ring-Opening and Its Impact on Solid Electrolyte Interphase Evolution. *J. Phys. Chem. C* **2019**, *123*, 17695−17702.
(61) Spotte-Smith, E. W. C.; Cohen, O. A.; Blau, S. M.; Munro, J. M.; Yang, R.; Guha, R. D.; Patel, H. D.; Vijay, S.; Huck, P.; Kingsbury, R.; Horton, M. K.; Persson, K. A. A Database of Molecular Properties Integrated in the Materials Project. *Digital Discovery* **2023**, *2*, 1862−1882.
(62) Spotte-Smith, E. W. C.; Vijay, S.; Petrocelli, T. B.; Rinkel, B. L. D.; McCloskey, B. D.; Persson, K. A. Data for "A Critical Analysis of Chemical and Electrochemical Oxidation Mechanisms in Li-Ion Batteries". 2023; Figshare, DOI: 10.6084/m9.figshare.24589056 (accessed 2023-12-18).
(63) Ong, S. P.; Richards, W. D.; Jain, A.; Hautier, G.; Kocher, M.; Cholia, S.; Gunter, D.; Chevrier, V. L.; Persson, K. A.; Ceder, G. Python Materials Genomics (Pymatgen): A Robust, Open-Source Python Library for Materials Analysis. *Comput. Mater. Sci.* **2013**, *68*, 314−319.
(64) Epifanovsky, E.; Gilbert, A. T. B.; Feng, X.; Lee, J.; Mao, Y.; Mardirossian, N.; Pokhilko, P.; White, A. F.; Coons, M. P.; Dempwolff, A. L.; Gan, Z.; Hait, D.; Horn, P. R.; Jacobson, L. D.; Kaliman, I.; Kussmann, J.; Lange, A. W.; Lao, K. U.; Levine, D. S.; Liu, J.; McKenzie, S. C.; Morrison, A. F.; Nanda, K. D.; Plasser, F.; Rehn, D. R.; Vidal, M. L.; You, Z.-Q.; Zhu, Y.; Alam, B.; Albrecht, B. J.; Aldossary, A.; Alguire, E.; Andersen, J. H.; Athavale, V.; Barton, D.; Begam, K.; Behn, A.; Bellonzi, N.; Bernard, Y. A.; Berquist, E. J.; Burton, H. G. A.; Carreras, A.; Carter-Fenk, K.; Chakraborty, R.; Chien, A. D.; Closser, K. D.; Cofer-Shabica, V.; Dasgupta, S.; de Wergifosse, M.; Deng, J.; Diedenhofen, M.; Do, H.; Ehlert, S.; Fang, P.-T.; Fatehi, S.; Feng, Q.; Friedhoff, T.; Gayvert, J.; Ge, Q.; Gidofalvi, G.; Goldey, M.; Gomes, J.; González-Espinoza, C. E.; Gulania, S.; Gunina, A. O.; Hanson-Heine, M. W. D.; Harbach, P. H. P.; Hauser, A.; Herbst, M. F.; Hernández Vera, M.; Hodecker, M.; Holden, Z. C.; Houck, S.; Huang, X.; Hui, K.; Huynh, B. C.; Ivanov, M.; Jász, Ã.; Ji, H.; Jiang, H.; Kaduk, B.; Kähler, S.; Khistyaev, K.; Kim, J.; Kis, G.; Klunzinger, P.; Koczor-Benda, Z.; Koh, J. H.; Kosenkov, D.; Koulias, L.; Kowalczyk, T.; Krauter, C. M.; Kue, K.; Kunitsa, A.; Kus, T.; Ladjánszki, I.; Landau, A.; Lawler, K. V.; Lefrancois, D.; Lehtola, S.; Li, R. R.; Li, Y.-P.; Liang, J.; Liebenthal, M.; Lin, H.-H.; Lin, Y.-S.; Liu, F.; Liu, K.-Y.; Loipersberger, M.; Luenser, A.; Manjanath, A.; Manohar, P.; Mansoor, E.; Manzer, S. F.; Mao, S.-P.; Marenich, A. V.; Markovich, T.; Mason, S.; Maurer, S. A.; McLaughlin, P. F.; Menger, M. F. S. J.; Mewes, J.-M.; Mewes, S. A.; Morgante, P.; Mullinax, J. W.; Oosterbaan, K. J.; Paran, G.; Paul, A. C.; Paul, S. K.; Pavošević, F.; Pei, Z.; Prager, S.; Proynov, E. I.; Rák, Ã.; Ramos-Cordoba, E.; Rana, B.; Rask, A. E.; Rettig, A.; Richard, R. M.; Rob, F.; Rossomme, E.; Scheele, T.; Scheurer, M.; Schneider, M.; Sergueev, N.; Sharada, S. M.; Skomorowski, W.; Small, D. W.; Stein, C. J.; Su, Y.-C.; Sundstrom, E. J.; Tao, Z.; Thirman, J.; Tornai, G. J.; Tsuchimochi, T.; Tubman, N. M.; Veccham, S. P.; Vydrov, O.; Wenzel, J.; Witte, J.; Yamada, A.; Yao, K.; Yeganeh, S.; Yost, S. R.; Zech, A.; Zhang, I. Y.; Zhang, X.; Zhang, Y.; Zuev, D.; Aspuru-Guzik, A.; Bell, A. T.; Besley, N. A.; Bravaya, K. B.; Brooks, B. R.; Casanova, D.; Chai, J.-D.; Coriani, S.; Cramer, C. J.; Cserey, G.; DePrince, A. E., III; DiStasio, R. A., Jr.; Dreuw, A.; Dunietz, B. D.; Furlani, T. R.; Goddard, W. A., III; Hammes-Schiffer, S.; Head-Gordon, T.; Hehre, W. J.; Hsu, C.-P.; Jagau, T.-C.; Jung, Y.; Klamt, A.; Kong, J.; Lambrecht, D. S.; Liang, W.; Mayhall, N. J.; McCurdy, C. W.; Neaton, J. B.; Ochsenfeld, C.; Parkhill, J. A.; Peverati, R.; Rassolov, V. A.; Shao, Y.; Slipchenko, L. V.; Stauch, T.; Steele, R. P.; Subotnik, J. E.; Thom, A. J. W.; Tkatchenko, A.; Truhlar, D. G.; Van Voorhis, T.; Wesolowski, T. A.; Whaley, K. B.; Woodcock, H. L., III; Zimmerman, P. M.; Faraji, S.; Gill, P. M. W.; Head-Gordon, M.; Herbert, J. M.; Krylov, A. I. Software for the Frontiers of Quantum Chemistry: An Overview of Qevelopments in the Q-Chem 5 Package. *J. Chem. Phys.* **2021**, *155*, No. 084801.
(65) Mardirossian, N.; Head-Gordon, M. B97X-V: A 10-parameter, Range-Separated Hybrid, Generalized Gradient Approximation Density Functional with Nonlocal Correlation, Designed by a Survival-of-the-Fittest Strategy. *Phys. Chem. Chem. Phys.* **2014**, *16*, 9904−9924.
(66) Rappoport, D.; Furche, F. Property-Optimized Gaussian Basis Sets for Molecular Response Calculations. *J. Chem. Phys.* **2010**, *133*, 134105.
(67) Marenich, A. V.; Cramer, C. J.; Truhlar, D. G. Universal Solvation Model Based on Solute Electron Density and on a Continuum Model of the Solvent Defined by the Bulk Dielectric Constant and Atomic Surface Tensions. *J. Phys. Chem. B* **2009**, *113*, 6378−6396.
(68) Spotte-Smith, E. W. C.; Blau, S. M.; Xie, X.; Patel, H. D.; Wen, M.; Wood, B.; Dwaraknath, S.; Persson, K. A. Quantum Chemical Calculations of Lithium-Ion Battery Electrolyte and Interphase Species. *Sci. Data* **2021**, *8*, 203.
(69) Mullinax, J. W.; Bauschlicher, C. W. J.; Lawson, J. W. Reaction of Singlet Oxygen with the Ethylene Group: Implications for Electrolyte Stability in Li-Ion and Li-O2 Batteries. *J. Phys. Chem. A* **2021**, *125*, 2876−2884.

https://doi.org/10.1021/acs.jpclett.3c03279
J. Phys. Chem. Lett. 2024, 15, 391−400

(70) Schweitzer, C.; Schmidt, R. Physical Mechanisms of Generation and Deactivation of Singlet Oxygen. *Chem. Rev.* **2003**, *103*, 1685−1758.
(71) Ervin, K. M.; Anusiewicz, I.; Skurski, P.; Simons, J.; Lineberger, W. C. The Only Stable State of O_2^- Is the X^2_g Ground State and It (Still!) Has an Adiabatic Electron Detachment Energy of 0.45 eV. *J. Phys. Chem. A* **2003**, *107*, 8521−8529.
(72) Read, J.; Mutolo, K.; Ervin, M.; Behl, W.; Wolfenstine, J.; Driedger, A.; Foster, D. Oxygen Transport Properties of Organic Electrolytes and Performance of Lithium/Oxygen Battery. *J. Electrochem. Soc.* **2003**, *150*, A1351.

https://doi.org/10.1021/acs.jpclett.3c03279
J. Phys. Chem. Lett. 2024, 15, 391−400